Available online at www.sciencedirect.com
SCIENCE DIRECT®

ELSEVIER

Journal of Computational Physics 192 (2003) 262–276

JOURNAL OF COMPUTATIONAL PHYSICS

www.elsevier.com/locate/jcp

A new class of truly consistent splitting schemes for incompressible flows

J.L. Guermond [a,1], Jie Shen [b,*,2]

[a] LIMSI (CNRS-UPR 3152), BP 133, 91403, Orsay, France
[b] Department of Mathematics, Purdue University, West Lafayette 47907, USA

Received 4 March 2003; received in revised form 14 July 2003; accepted 15 July 2003

Abstract

A new class of splitting schemes for incompressible flows is introduced. The new schemes are based on a weak form of the pressure Poisson equation and, at each time step, only require to solve a set of Helmholtz-type equations for the velocity and a Poisson equation (in the weak form) for the pressure, just as pressure-correction and velocity-correction schemes. However, unlike pressure-correction and velocity-correction schemes, the new splitting schemes are free of splitting errors and deliver full accuracy on the vorticity and the pressure.

AMS: 76D05; 65M12; 65M60

Keywords: Navier–Stokes equations; Projection methods; Fractional step methods; Incompressibility; Finite elements; Spectral approximations

1. Introduction

We consider in this paper the time discretization of the unsteady incompressible Navier–Stokes equations in primitive variables. For a given body force $\boldsymbol{f}$, we look for $\boldsymbol{u}$ and p such that

$$\begin{cases} \boldsymbol{u}_t - \nu\nabla^2\boldsymbol{u} + \boldsymbol{u}\cdot\nabla\boldsymbol{u} + \nabla p = \boldsymbol{f} & \text{in } \Omega\times(0,T], \\ \nabla\cdot\boldsymbol{u} = 0 \quad \text{in } \Omega\times[0,T], \end{cases} \tag{1.1}$$

* Corresponding author. Tel.: +1-765-494-1923.
E-mail addresses: guermond@limsi.fr (J.L. Guermond), shen@math.purdue.edu (J. Shen).
[1] The work of this author is supported by CNRS and Texas Institute for Computational and Applied Mathematics, Austin, Texas, under TICAM Visiting Faculty Fellowships. Part of the work was completed while this author was visiting the University of Central Florida and Purdue University.
[2] The work of this author is partially supported by NFS Grant DMS-0074283.

0021-9991/$ - see front matter
doi:10.1016/j.jcp.2003.07.009

subject to appropriate initial and boundary conditions for $\boldsymbol{u}$. Ω is an open and bounded domain in $\mathbb{R}^d$ ($d = 2$ or 3 in practical situations) and $[0, T]$ is the time interval.

Since the introduction of the concept of projection methods by Chorin [5] and Temam [24] in the late 1960s, there have been an enormous body of work devoted to the analysis and implementation of various versions of these techniques. The various improvements on the original scheme by Chorin and Temam can be roughly classified into two broad categories, namely the pressure-correction techniques and the velocity-correction techniques.

• The idea of pressure-correction methods can be traced back to [8] in the form of a first-order scheme. Pressure-correction schemes are time marching algorithms with two substeps. The pressure is made explicit in the first sub-step, and is corrected in the second sub-step by projecting the intermediate velocity onto the space of divergence-free vector field. This strategy became a popular choice after Van Kan (cf. [27]) proposed a (formally) second-order version which dramatically improved the accuracy. This second-order pressure-correction scheme is further improved by adding a divergence correction to the pressure [26]. This improved version is classified in [15] as the rotational form of the pressure-correction schemes. This class of schemes are now widely used in practice and have been rigorously analyzed in [4,6,11,22,23]. In passing we want to point out that the scheme proposed by Kim and Moin (cf. [18]) can also be reformulated as the pressure-correction scheme in the rotational form. This fact does not seem to be well-known.

• The notion of velocity-correction schemes was first introduced by the authors in [13]. In a velocity-correction scheme, the viscous term is made explicit in the first sub-step and the velocity is corrected in the second sub-step. It is shown in [13] that the class of fractional step schemes introduced by Orszag et al. [19] and Karniadakis et al. [16] can be reformulated as a velocity-correction scheme in rotational form. The notion of third-order BDF and higher-order splitting scheme has been introduced in [16]. We note in passing that while third or higher-order pressure-correction schemes become unstable (cf. [20]), ample numerical evidences (cf. [16,17]) indicate that third or higher-order velocity-correction schemes in rotational form are stable. This behavior has yet to be fully explain.

The main advantage of projection-type algorithms is that the computations of the velocity and the pressure are decoupled. More precisely, assuming that the nonlinear terms are made explicit, then at each time step, one only has to solve a set of Helmholtz-type equations for the velocity and a scalar Poisson equation (with a homogeneous Neumann boundary condition) for the pressure. This strategy is computationally very efficient when compared with the coupled approach, especially when a fast Poisson solver is available. However, the price for the decoupling is some loss of accuracy on the pressure and the vorticity. More precisely, the so-called second-order projection schemes provide second-order accuracy on the velocity in the L^2-norm, while the convergence rates of the pressure and the vorticity in the L^2-norm are either first-order or $3/2$-order depending on whether it is the standard form or the rotational form which is used (cf. [13,15]). Since the vorticity (and oftentimes the pressure) plays a very important role in applications, it is highly desirable to have a decoupled scheme which is unconditionally stable (for the time-dependent Stokes equations) and provides full second-order accuracy for both the vorticity and the pressure. The aim of this paper is to introduce such a scheme. We note that the gauge method introduced by E and Liu [7] with a finite difference discretization is reported to numerically achieve full second-order accuracy on the velocity and the gauge variable, but the proof of this conjecture is still missing. Moreover, when needed, the pressure is computed by using $p = \partial_t\phi - \mu\Delta\phi$, where ϕ is the gauge variable. Hence, it is not easy to obtain an accurate pressure approximation, especially in the context of finite-elements.

The rest of the paper is organized as follows. In Section 2 we define some notations, and we introduce the new class of splitting techniques. Two variants are considered; these variants are hereafter called the standard formulation and the rotational formulation. We analyze the stability and the convergence properties of the standard and rotational variants in Section 3. In Section 4, we briefly explain the role of the inf-sup condition when these schemes are discretized in space. Convergence tests and various numerical experiments are reported in Section 5.

2. A new class of splitting schemes

2.1. Some notations

Let $\Delta t > 0$ be a time step and set $t_k = k\Delta t$ for $0 \leqslant k \leqslant K = [T/\Delta t]$. Let $\phi^0, \phi^1, \ldots, \phi^K$ be a sequence of functions in some Banach space E with norm $\|\cdot\|_E$. We denote by $\phi_{\Delta t}$ this sequence, and we shall use the following discrete norms:

$$\|\phi_{\Delta t}\|_{\ell^2(E)} := \left(\Delta t \sum_{k=0}^{K} \|\phi^k\|_E^2\right)^{1/2}, \quad \|\phi_{\Delta t}\|_{\ell^\infty(E)} := \max_{0\leqslant k\leqslant K}\left(\|\phi^k\|_E^2\right). \tag{2.1}$$

Let $L^2(\Omega)$ (resp. $L^2(\Omega)^d$) be the set of square integrable scalar-valued (resp. vector-valued) functions. We denote the scalar product in $L^2(\Omega)$ and $L^2(\Omega)^d$ by $(\cdot,\cdot)$ without making a distinction between scalar- and vector-valued functions. We will denote $\|\cdot\|_E$ by $\|\cdot\|$ when $E = L^2(\Omega)$.

We denote by C a generic constant which is independent Δt but possibly depends on the data and the solution. We shall also use the expression $A \lesssim B$ to say that there exists a generic constant c such that $A \leqslant cB$.

To avoid unnecessary technical difficulties associated with non-homogeneous Dirichlet conditions, we assume that $\boldsymbol{u}$ is zero at the boundary of the domain, henceforth denoted by Γ.

2.2. The key idea

The key idea behind the new class of splitting schemes is to evaluate the pressure by testing the momentum equation against gradients. By taking the L^2-inner product of the momentum equation in (1.1) with ∇q and noticing that $(\boldsymbol{u}_t, \nabla q) = -(\nabla\cdot\boldsymbol{u}_t, q) = 0$, we obtain

$$\int_\Omega \nabla p\cdot\nabla q = \int_\Omega (\boldsymbol{f} + \nabla^2\boldsymbol{u} - \boldsymbol{u}\cdot\nabla\boldsymbol{u})\cdot\nabla q, \quad \forall q \in H^1(\Omega). \tag{2.2}$$

Note that if $\boldsymbol{u}$ is known, (2.2) is simply the weak form of a Poisson equation for the pressure. So, the principle we shall follow is to compute the velocity and the pressure in two consecutive steps: First, we compute the velocity by making explicit the pressure, then we update the pressure by making use of (2.2).

Following [16], we use the qth-order backward difference formula (BDFq) to approximate $\partial_t\boldsymbol{v}(t^{k+1})$ and the qth order extrapolation to approximate $p(t_{k+1})$. These approximations are denoted by

$$\frac{1}{\Delta t}\left(\beta_q\boldsymbol{v}^{k+1} - \sum_{j=0}^{q-1}\beta_j\boldsymbol{v}^{k-j}\right)$$

and

$$p^{\star,k+1} = \sum_{j=0}^{q-1}\gamma_j p^{k-j},$$

respectively. Of course, the present theory is not restricted to these choices. Any implicit consistent approximation of $\partial_t\boldsymbol{v}(t^{k+1})$ and any explicit consistent approximation of $p(t_{k+1})$ is acceptable; see scheme (2.13)–(2.15) for instance. To simplify the notation, for any sequence $\phi_{\Delta t} := (\phi^0, \phi^1, \ldots)$, we set

$$D\phi^{k+1} = \beta_q\phi^{k+1} - \sum_{j=0}^{q-1}\beta_j\phi^{k-j}.$$

For instance, we have

$$
\begin{aligned}
q=1:&\ \ D\boldsymbol{v}^{k+1}=\boldsymbol{v}^{k+1}-\boldsymbol{v}^{k}, && p^{\star,k+1}=p^{k};\\
q=2:&\ \ D\boldsymbol{v}^{k+1}=\tfrac{3}{2}\boldsymbol{v}^{k+1}-2\boldsymbol{v}^{k}+\tfrac{1}{2}\boldsymbol{v}^{k-1}, && p^{\star,k+1}=2p^{k}-p^{k-1}.
\end{aligned}
\tag{2.3}
$$

2.3. Standard splitting scheme

A qth order *decoupled* approximation to (1.1) is defined as follows: Let $\boldsymbol{u}^0=\boldsymbol{u}|_{t=0}$ and $p^0=p|_{t=0}$ (which can be obtained by solving (2.2) at $t=0$). If $q\geqslant 2$, then for $1\leqslant k\leqslant q-1$, let $(\boldsymbol{u}^k,p^k)$ be the kth order approximation to $(\boldsymbol{u}(k\Delta t),p(k\Delta t))$ (which can be obtained recursively by using the scheme described below using BDFk and the kth order extrapolation of the pressure). Let us denote by $\boldsymbol{g}^{k+1}$ the difference between $\boldsymbol{f}\ (t^{k+1})$ and an appropriate q-th order approximation of the nonlinear term, say $\boldsymbol{g}^{k+1}=\boldsymbol{f}\ (t^{k+1})-(\boldsymbol{u}\cdot\nabla\boldsymbol{u})^{\star,k+1}$. Then, for $k\geqslant q-1$, find $\boldsymbol{u}^{k+1}$ and p^{k+1} such that

$$
\frac{D\boldsymbol{u}^{k+1}}{\Delta t}-\nu\nabla^2\boldsymbol{u}^{k+1}+\nabla p^{\star,k+1}=\boldsymbol{g}^{k+1},\quad \boldsymbol{u}^{k+1}|_{\Gamma}=0,\tag{2.4}
$$

$$
(\nabla p^{k+1},\nabla q)=(\boldsymbol{g}^{k+1}+\nu\nabla^2\boldsymbol{u}^{k+1},\nabla q),\quad \forall q\in H^1(\Omega).\tag{2.5}
$$

Note that in the second step we need to compute $\nabla^2\boldsymbol{u}^{k+1}$ which may not be well defined in a finite element discretization. Hence, we shall derive an alternative formulation which does not require computing $\nabla^2\boldsymbol{u}^{k+1}$ and is more suitable for finite element discretizations. To this end, we take the inner product of the first step with ∇q and we subtract the result from the second step. Then, we obtain the following equivalent formulation of (2.4) and (2.5):

$$
\frac{D\boldsymbol{u}^{k+1}}{\Delta t}-\nu\nabla^2\boldsymbol{u}^{k+1}+\nabla p^{\star,k+1}=\boldsymbol{g}^{k+1},\quad \boldsymbol{u}^{k+1}|_{\Gamma}=0,\tag{2.6}
$$

$$
(\nabla(p^{k+1}-p^{\star,k+1}),\nabla q)=\left(\frac{D\boldsymbol{u}^{k+1}}{\Delta t},\nabla q\right),\quad \forall q\in H^1(\Omega).\tag{2.7}
$$

At this stage, several remarks are in order.

- The two schemes (2.4) and (2.5) and (2.6) and (2.7) are strictly equivalent in the space continuous case but they yield two different series of implementations when the space variables are discretized (see Section 4 for further details).
- Neither scheme (2.4) and (2.5) nor (2.6) and (2.7) is a projection scheme, for the velocity approximation $\boldsymbol{u}^{k+1}$ is not divergence-free.
- As in a projection scheme, one only needs to solve a set of Helmholtz-type equations for $\boldsymbol{u}^{k+1}$ and a Poisson equation (2.5) or (2.7) (in the weak form) for p^{k+1}.
- Just as in a pressure-correction scheme in standard form [15], the Eq. (2.7) implies that $\frac{\partial}{\partial\boldsymbol{n}}(p^{k+1}-p^{\star,k+1})|_{\partial\Omega}=0$ which is an artificial Neumann boundary condition not satisfied by the exact pressure. This boundary condition will induce a numerical boundary layer which, in turn, will result in a loss of accuracy.

2.4. Consistent splitting scheme

Similarly to pressure-correction and velocity-correction schemes (cf. [13–16,19,26]), the accuracy of the above splitting schemes can be improved by replacing $\nabla^2\boldsymbol{u}^{k+1}$ in (2.5) by $-\nabla\times\nabla\times\boldsymbol{u}^{k+1}$, leading to the following algorithm:

$$\frac{D\boldsymbol{u}^{k+1}}{\Delta t} - \nu\nabla^2\boldsymbol{u}^{k+1} + \nabla p^{\star,k+1} = \boldsymbol{g}^{k+1}, \ \boldsymbol{u}^{k+1}|_\Gamma = 0, \tag{2.8}$$

$$(\nabla p^{k+1}, \nabla q) = (\boldsymbol{g}^{k+1} - \nu\nabla\times\nabla\times\boldsymbol{u}^{k+1}, \nabla q), \ \forall q \in H^1(\Omega). \tag{2.9}$$

Owing to the identity $\nabla^2\boldsymbol{u}^{k+1} = \nabla\nabla\cdot\boldsymbol{u}^{k+1} - \nabla\times\nabla\times\boldsymbol{u}^{k+1}$, this procedure amounts to removing the term $\nabla\nabla\cdot\boldsymbol{u}^{k+1}$ in (2.5). It is shown in [13,15] that when this strategy is applied to pressure-correction and velocity-correction schemes, it yields an a priori control on the divergence of $\boldsymbol{u}^{k+1}$, which in turn leads to improved accuracy on the vorticity and the pressure. Once again, to avoid computing $\nabla\times\nabla\times\boldsymbol{u}^{k+1}$ explicitly in the second step, we take the inner product of (2.8) with ∇q and we subtract the result from (2.9). This leads to an equivalent alternative form of (2.8) and (2.9) (the equivalence holds only in the space continuous case):

$$\frac{D\boldsymbol{u}^{k+1}}{\Delta t} - \nu\nabla^2\boldsymbol{u}^{k+1} + \nabla p^{\star,k+1} = \boldsymbol{g}^{k+1}, \ \boldsymbol{u}^{k+1}|_\Gamma = 0, \tag{2.10}$$

$$(\nabla\psi^{k+1}, \nabla q) = \left(\frac{D\boldsymbol{u}^{k+1}}{\Delta t}, \nabla q\right), \ \forall q \in H^1(\Omega). \tag{2.11}$$

$$p^{k+1} = \psi^{k+1} + p^{\star,k+1} - \nu\nabla\cdot\boldsymbol{u}^{k+1}. \tag{2.12}$$

Note that the numerical complexity of the schemes (2.8) and (2.9) and (2.10)–(2.12) is the same as that of (2.4) and (2.5) or (2.6) and (2.7). However, as ample numerical results indicate, the pressure approximation p^{k+1} is no longer plagued by an artificial Neumann boundary condition and, consequently, these schemes provide truly qth order accuracy (at least for $q = 1$ and 2) for the velocity, vorticity and pressure. Thus, we shall henceforth refer to the schemes (2.8) and (2.9) and (2.10)–(2.12) as the *consistent splitting* schemes.

As already mentioned in Section 2.2, the use of a BDF approximation for $\partial_t\boldsymbol{u}$ and of an extrapolation for p is not really a key issue. In fact, one can build another truly second-order consistent splitting scheme by using the Crank–Nicolson and leap-frog strategy as follows: first compute $\boldsymbol{u}^{k+1}$ such that

$$\frac{\boldsymbol{u}^{k+1} - \boldsymbol{u}^{k-1}}{2\Delta t} - \frac{\nu}{2}\nabla^2(\boldsymbol{u}^{k+1} + \boldsymbol{u}^{k-1}) + \nabla p^k = \boldsymbol{g}^k, \quad \boldsymbol{u}^{k+1}|_\Gamma = 0,$$

then compute the pressure by testing the momentum equation against gradients

$$\left(\nabla\frac{1}{2}(p^{k+1} + p^{k-1}), \nabla q\right) = \left(\boldsymbol{g}^k - \frac{\nu}{2}\nabla\times\nabla\times(\boldsymbol{u}^{k+1} + \boldsymbol{u}^{k-1}), \nabla q\right), \quad \forall q \in H^1(\Omega).$$

We can avoid having to test gradients against second-order derivatives by testing the equation controlling $\boldsymbol{u}^{k+1}$ against gradients and subtracting the result from the above equation. The resulting algorithm is as follows:

$$\frac{\boldsymbol{u}^{k+1} - \boldsymbol{u}^{k-1}}{2\Delta t} - \frac{\nu}{2}\nabla^2(\boldsymbol{u}^{k+1} + \boldsymbol{u}^{k-1}) + \nabla p^k = \boldsymbol{g}^k, \quad \boldsymbol{u}^{k+1}|_\Gamma = 0, \tag{2.13}$$

$$(\nabla\psi^{k+1}, \nabla q) = \left(\frac{\boldsymbol{u}^{k+1} - \boldsymbol{u}^{k-1}}{2\Delta t}, \nabla q\right), \quad \forall q \in H^1(\Omega), \tag{2.14}$$

$$p^{k+1} = 2\psi^{k+1} + 2p^k - p^{k-1} - \nu\nabla\cdot(\boldsymbol{u}^{k+1} + \boldsymbol{u}^k). \tag{2.15}$$

3. Stability and convergence results

Since the nonlinear term does not contribute in any essential way to the error analysis of projection methods, we shall carry out our analysis for the linearized equations only so as to avoid technicalities which may obscure the essential ideas in the proof. Our proofs can be adapted to account for the nonlinearity using standard techniques (cf. [11,22,25]).

3.1. Standard splitting schemes

Let us first show that the solution of the second-order version of (2.6) and (2.7) is unconditionally bounded. Since the use of second-order BDF in (2.6) does not affect the stability in an essential manner and the additional technicalities involved with the second-order BDF have already been addressed in [13,15], for the sake of simplicity, we will replace the second-order BDF in (2.6) by the backward Euler approximation, i.e., we consider

$$\frac{\boldsymbol{u}^{k+1}-\boldsymbol{u}^k}{\Delta t} - \nu\nabla^2\boldsymbol{u}^{k+1} + \nabla(2p^k - p^{k-1}) = \boldsymbol{g}^{k+1}, \quad \boldsymbol{u}^{k+1}|_\Gamma = 0, \tag{3.1}$$

$$(\nabla(p^{k+1} - 2p^k + p^{k-1}), \nabla q) = \left(\frac{\boldsymbol{u}^{k+1}-\boldsymbol{u}^k}{\Delta t}, \nabla q\right), \quad \forall q \in H^1(\Omega). \tag{3.2}$$

Let us denote the backward difference operator by δ, i.e., $\delta\boldsymbol{u}^{k+1} = \boldsymbol{u}^{k+1} - \boldsymbol{u}^k$ and $\delta p^{k+1} = p^{k+1} - p^k$. The operators δ^2, δ^3 are defined accordingly.

Lemma 3.1. *There exists a positive constant C such that the solution of* (3.1) *and* (3.2) *is bounded in the following sense:*

$$\|\delta\boldsymbol{u}^{n+1}\|^2 + \Delta t^2\|\nabla\delta p^{n+1}\|^2 + \Delta t\sum_{k=1}^{n}(\nu\|\nabla\delta\boldsymbol{u}^{k+1}\|^2 + \Delta t\|\nabla\delta^2 p^k\|^2) \leqslant C.$$

Proof. Applying the operator δ to (3.1) and (3.2), we find

$$\frac{\delta^2\boldsymbol{u}^{k+1}}{\Delta t} - \nu\nabla^2\delta\boldsymbol{u}^{k+1} + \nabla(\delta p^k + \delta^2 p^k) = \delta\boldsymbol{g}^{k+1}, \quad \delta\boldsymbol{u}^{k+1}|_\Gamma = 0, \tag{3.3}$$

and

$$(\nabla\delta^3 p^{k+1}, \nabla q) = \left(\frac{\delta^2\boldsymbol{u}^{k+1}}{\Delta t}, \nabla q\right), \quad \forall q \in H^1(\Omega). \tag{3.4}$$

Taking the inner product of (3.3) with $2\Delta t\delta\boldsymbol{u}^{k+1}$ in $L^2(\Omega)$, using the identity $(a-b, 2a) = |a|^2 - |b|^2 + |a-b|^2$, and integrating by parts, we obtain

$$\|\delta\boldsymbol{u}^{k+1}\|^2 - \|\delta\boldsymbol{u}^k\|^2 + \|\delta^2\boldsymbol{u}^{k+1}\|^2 + 2\nu\Delta t\|\nabla\delta\boldsymbol{u}^{k+1}\|^2 + 2\Delta t(\nabla(\delta p^k + \delta^2 p^k), \delta\boldsymbol{u}^{k+1}) = 2\Delta t(\delta\boldsymbol{g}^{k+1}, \delta\boldsymbol{u}^{k+1}). \tag{3.5}$$

Next, we take $q = 2\Delta t^2\delta p^k$ in (3.2) to get

$$\Delta t^2(\|\nabla\delta p^{k+1}\|^2 - \|\nabla\delta p^k\|^2 - \|\nabla\delta^2 p^{k+1}\|^2) = 2\Delta t(\delta\boldsymbol{u}^{k+1}, \nabla\delta p^k). \tag{3.6}$$

Similarly, by taking $q = 2\Delta t^2\delta^2 p^k$ in (3.2), we obtain

$$\Delta t^2(\|\nabla\delta^2 p^{k+1}\|^2 + \|\nabla\delta^2 p^k\|^2 - \|\nabla\delta^3 p^{k+1}\|^2) = 2\Delta t(\delta\boldsymbol{u}^{k+1}, \nabla\delta^2 p^k). \tag{3.7}$$

On the other hand, we derive from (3.4) that

$$\Delta t^2\|\nabla\delta^3 p^{k+1}\|^2 \leqslant \|\delta^2\boldsymbol{u}^{k+1}\|^2. \tag{3.8}$$

Summing up the last four relations (3.5)–(3.8), we obtain

$$\begin{aligned}&\|\delta\boldsymbol{u}^{k+1}\|^2 - \|\delta\boldsymbol{u}^k\|^2 + 2\nu\Delta t\|\nabla\delta\boldsymbol{u}^{k+1}\|^2 + \Delta t^2(\|\nabla\delta^2 p^k\|^2 + \|\nabla\delta p^{k+1}\|^2 - \|\nabla\delta p^k\|^2)\\ &\quad\leqslant 2\Delta t(\delta\boldsymbol{g}^{n+1}, \delta\boldsymbol{u}^{n+1}) \leqslant \nu\Delta t\|\nabla\delta\boldsymbol{u}^{k+1}\|^2 + \frac{c_1^2}{\nu}\Delta t\|\delta\boldsymbol{g}^{n+1}\|^2.\end{aligned} \tag{3.9}$$

The last inequality in the above relation is the result of the Poincaré inequality $\|\delta\boldsymbol{u}^{k+1}\| \leqslant c_1\|\nabla\delta\boldsymbol{u}^{k+1}\|$ and the Cauchy–Schwarz inequality.

Finally, we take the sum of (3.9) for $k = 1$ to n to arrive at

$$\begin{aligned}&\|\delta\boldsymbol{u}^{n+1}\|^2 + \Delta t^2\|\nabla\delta p^{n+1}\|^2 + \Delta t\sum_{k=1}^{n}(\nu\|\nabla\delta\boldsymbol{u}^{k+1}\|^2 + \Delta t\|\nabla\delta^2 p^k\|^2)\\ &\quad\leqslant \frac{c_1^2}{\nu}\Delta t\sum_{k=1}^{n}\|\delta\boldsymbol{g}^{n+1}\|^2 + \|\delta\boldsymbol{u}^1\|^2 + \|\nabla\delta p^1\|^2 \leqslant C.\end{aligned}$$

This completes the proof. □

The above lemma shows that the solution of the algorithms (2.6) and (2.7) with $q = 2$ is unconditionally bounded. In fact, we can prove the following error estimates for (2.6) and (2.7) with $q = 2$ (cf. [12]).

Theorem 3.1. *Provided that the solution to* (1.1) *is smooth enough in time and space, the solution* $(u_{\Delta t}, p_{\Delta t})$ *to* (2.6) *and* (2.7) *satisfies the estimates:*

$$\begin{aligned}&\|\boldsymbol{u}_{\Delta t} - u_{\Delta t}\|_{\ell^2(L^2(\Omega)^d)} \lesssim \Delta t^2,\\ &\|\boldsymbol{u}_{\Delta t} - u_{\Delta t}\|_{\ell^\infty(H^1(\Omega)^d)} + \|p_{\Delta t} - p_{\Delta t}\|_{\ell^\infty(L^2(\Omega))} \lesssim \Delta t.\end{aligned}$$

We note that the above error estimates are of the same order as those from the second-order pressure-correction scheme in standard form (cf. [11,22]), but they are less accurate than those from the second-order pressure-correction scheme in rotational form (cf. [13]).

3.2. Consistent splitting schemes

The analysis of the stability and the convergence of the consistent splitting scheme is more involved than that of the standard form. For the time being, we are only able to prove optimal convergence results with $q = 1$ (cf. [12]).

Theorem 3.2. *Provided that the solution to* (1.1) *is smooth enough in time and space, the solution* $(u_{\Delta t}, p_{\Delta t})$ *of* (2.10)–(2.12) *with* $q = 1$ *is unconditionally bounded and satisfies the following error estimates*

$$\|\boldsymbol{u}_{\Delta t} - u_{\Delta t}\|_{\ell^\infty(H^1(\Omega)^d)} + \|p_{\Delta t} - p_{\Delta t}\|_{\ell^\infty(L^2(\Omega))} \lesssim \Delta t.$$

Since a complete proof of this theorem is beyond the scope of this paper, we only give a proof for the stability. Heuristically speaking, a combination of the stability result proved below and the consistency error of the scheme (easily available from a Taylor expansion) implies the above error estimates.

Proof (*Proof of stability*). For $q = 1$, the scheme (2.10)–(2.12) reads

$$\frac{\boldsymbol{u}^{k+1} - \boldsymbol{u}^k}{\Delta t} - v\Delta \boldsymbol{u}^{k+1} + \nabla p^k = \boldsymbol{g}^{k+1}, \ \boldsymbol{u}^{k+1}|_\Gamma = 0; \tag{3.10}$$

$$(\nabla \psi^{k+1}, \nabla q) = \left(\frac{\boldsymbol{u}^{k+1} - \boldsymbol{u}^k}{\Delta t}, \nabla q\right), \ \forall q \in H^1(\Omega), \tag{3.11}$$

$$p^{k+1} = \psi^{k+1} + p^k - v\nabla \cdot \boldsymbol{u}^{k+1}. \tag{3.12}$$

Applying the operator δ to (3.10) and using the identity $-\Delta \boldsymbol{u} = \nabla \times \nabla \times \boldsymbol{u} - \nabla\nabla \cdot \boldsymbol{u}$, we obtain

$$\frac{\delta^2 \boldsymbol{u}^{k+1}}{\Delta t} + v\nabla \times \nabla \times \delta \boldsymbol{u}^{k+1} - v\nabla\nabla \cdot \boldsymbol{u}^{k+1} + \nabla \psi^k = \delta \boldsymbol{g}^{k+1}. \tag{3.13}$$

Taking the inner product of (3.13) with $2\Delta t \delta \boldsymbol{u}^{k+1}$ and integrating by parts, we have

$$\begin{aligned} &\|\delta \boldsymbol{u}^{k+1}\|^2 - \|\delta \boldsymbol{u}^k\|^2 + \|\delta^2 \boldsymbol{u}^{k+1}\|^2 + v\Delta t(\|\nabla \cdot \boldsymbol{u}^{k+1}\|^2 - \|\nabla \cdot \boldsymbol{u}^k\|^2 + \|\nabla \cdot \delta \boldsymbol{u}^{k+1}\|^2) \\ &\quad + 2v\Delta t\|\nabla \times \delta \boldsymbol{u}^{k+1}\|^2 + 2\Delta t(\nabla \psi^k, \delta \boldsymbol{u}^{k+1}) \\ &\qquad = 2\Delta t(\delta \boldsymbol{g}^{k+1}, \delta \boldsymbol{u}^{k+1}). \end{aligned} \tag{3.14}$$

We then apply the operator δ to (3.11) and take the scalar product with gradients to obtain

$$(\nabla \delta \psi^{k+1}, \nabla q) = \left(\frac{\delta \boldsymbol{u}^{k+1} - \delta \boldsymbol{u}^k}{\Delta t}, \nabla q\right), \ \forall q \in H^1(\Omega). \tag{3.15}$$

Taking $q = 2\Delta t^2 \psi^k$ in the above relation, we find

$$\Delta t^2(\|\nabla \psi^{k+1}\|^2 - \|\nabla \psi^k\|^2 - \|\nabla \delta \psi^{k+1}\|^2) = 2\Delta t(\delta \boldsymbol{u}^{k+1} - \delta \boldsymbol{u}^k, \nabla \psi^k). \tag{3.16}$$

We now take $q = 2\Delta t^2 \psi^{k+1}$ in (3.11), and we replace $k + 1$ by k to obtain

$$2\Delta t^2\|\nabla \psi^k\|^2 = 2\Delta t(\delta \boldsymbol{u}^k, \nabla \psi^k). \tag{3.17}$$

Next, we take $q = \Delta t^2 \delta \psi^{k+1}$ in (3.15), and we use the Cauchy–Schwarz inequality to find

$$\Delta t^2\|\nabla \delta \psi^{k+1}\|^2 \leqslant \|\delta^2 \boldsymbol{u}^{k+1}\|^2. \tag{3.18}$$

Summing up (3.14) and (3.16)–(3.18), and using the identity $\|\nabla \boldsymbol{u}\|^2 = \|\nabla \times \boldsymbol{u}\|^2 + \|\nabla \cdot \boldsymbol{u}\|^2$, which holds for all $\boldsymbol{u} \in H_0^1(\Omega)^d$, we obtain

$$\begin{aligned} &\|\delta \boldsymbol{u}^{k+1}\|^2 - \|\delta \boldsymbol{u}^k\|^2 + v\Delta t(\|\nabla \cdot \boldsymbol{u}^{k+1}\|^2 - \|\nabla \cdot \boldsymbol{u}^k\|^2) + v\Delta t(\|\nabla \delta \boldsymbol{u}^{k+1}\|^2 + \|\nabla \times \delta \boldsymbol{u}^{k+1}\|^2) \\ &\quad + \Delta t^2(\|\nabla \psi^{k+1}\|^2 + \|\nabla \psi^k\|^2) \\ &\qquad = 2\Delta t(\delta \boldsymbol{g}^{k+1}, \delta \boldsymbol{u}^{k+1}) \leqslant \frac{v\Delta t}{2}\|\nabla \delta \boldsymbol{u}^{k+1}\|^2 + \frac{4c_1^2\Delta t}{v}\|\delta \boldsymbol{g}^{k+1}\|^2. \end{aligned} \tag{3.19}$$

Finally, taking the sum of the above relation from $k = 1$ to n, we obtain

$$\|\delta \boldsymbol{u}^{n+1}\|^2 + \Delta t\|\nabla \cdot \boldsymbol{u}^{n+1}\|^2 + \Delta t\sum_{k=1}^{n}\left(\frac{v}{2}\|\nabla\delta \boldsymbol{u}^{k+1}\|^2 + \Delta t\|\nabla\psi^{k+1}\|^2\right)$$
$$\leqslant \frac{4c_1^2}{v}\Delta t\sum_{k=1}^{n}\|\delta \boldsymbol{g}^{n+1}\|^2 + \|\delta \boldsymbol{u}^1\|^2 + \Delta t\|\nabla \cdot \boldsymbol{u}^1\|^2 \leqslant C.$$

Hence, the solution of (3.10)–(3.12) is unconditionally bounded. □

Numerical results reported in Section 5 clearly indicate that the scheme with $q = 2$ is unconditionally stable and fully second-order for the velocity in the H^1-norm and the pressure in the L^∞-norm. However, a rigorous proof of this fact is still elusive.

4. Role of inf-sup conditions

Let (X_h, M_h) be respectively the approximation spaces for the velocity and the pressure. In this framework, the mixed approximation of the Stokes equations

$$-\Delta \boldsymbol{u} + \nabla p = \boldsymbol{f}, \quad \nabla \cdot \boldsymbol{u} = 0, \quad \boldsymbol{u}|_\Gamma = 0, \tag{4.1}$$

is as follows: Find $(\boldsymbol{u}_h, p_h) \in X_h \times M_h$ such that

$$\begin{aligned}&(\nabla \boldsymbol{u}_h, \nabla \boldsymbol{v}_h) - (p_h, \nabla \cdot \boldsymbol{v}_h) = (\boldsymbol{f}, \boldsymbol{v}_h), \quad \forall \boldsymbol{v}_h \in X_h,\\ &(\nabla \cdot \boldsymbol{u}_h, q_h) = 0, \quad \forall q_h \in M_h.\end{aligned} \tag{4.2}$$

It is now a well-known fact that a necessary condition for the above discrete problem to be well-posed is that the following inf-sup condition holds (cf. [2,3]):

$$\exists c_h > 0, \qquad \inf_{q_h \in M_h} \sup_{\boldsymbol{v}_h \in X_h} \frac{(q_h, \nabla \cdot \boldsymbol{v}_h)}{\|\nabla \boldsymbol{v}_h\| \, \|q_h\|} \geqslant c_h > 0. \tag{4.3}$$

Furthermore, if c_h is not uniformly bounded from below w.r.t h, a loss of accuracy of order c_h may occur on the velocity and a loss of order c_h^2 may occur on the pressure. On the other hand, if (4.3) is not satisfied, then the space of spurious pressure modes

$$Q_h = \{q_h \in M_h : (q_h, \nabla \cdot \boldsymbol{v}_h) = 0, \ \forall \boldsymbol{v}_h \in X_h\} \tag{4.4}$$

is not empty.

Since the computations of the velocity and the pressure approximations are decoupled in projection-type schemes, it is tempting to speculate, and it has been claimed by many, that the inf-sup condition between the velocity and the pressure approximation spaces is not mandatory for projection-type algorithms to work properly. In general, this intuitive argument is wrong. For instance, it is shown in [1,9] that the inf-sup condition is required to obtain optimal (in space) pressure error estimates in pressure-correction schemes. As for velocity-correction schemes, the situation is slightly more subtle and depends on how the scheme is implemented in practice.

The goal of this section is to elucidate the role of the inf-sup condition for the consistent splitting schemes.

4.1. Full discretization of (2.10)–(2.12)

Let us first consider the scheme (2.10)–(2.12). Let $X_h \subset H_0^1(\Omega)^d$, $W_h \subset H^1(\Omega)$, and $M_h \subset L^2(\Omega)$ be the approximation spaces for $\boldsymbol{u}_h^{k+1}$, ψ_h^{k+1}, and p_h^{k+1}, respectively. Then, a fully discretized version of (2.10)–(2.12) is: Find $(\boldsymbol{u}_h^{k+1}, \psi_h^{k+1}, p_h^{k+1}) \in X_h \times W_h \times M_h$ such that

$$\left(\frac{D\boldsymbol{u}_h^{k+1}}{\Delta t}, \boldsymbol{v}_h\right) + \nu\left(\nabla \boldsymbol{u}_h^{k+1}, \nabla \boldsymbol{v}_h\right) - \left(p_h^{\star,k+1}, \nabla \cdot \boldsymbol{v}_h\right) = (\boldsymbol{g}^{k+1}, \boldsymbol{v}_h), \quad \forall \boldsymbol{v}_h \in X_h, \tag{4.5}$$

$$\left(\nabla \psi_h^{k+1}, \nabla \phi_h\right) = \left(\frac{D\boldsymbol{u}_h^{k+1}}{\Delta t}, \nabla \phi_h\right), \quad \forall \phi_h \in W_h, \tag{4.6}$$

$$\left(p_h^{k+1}, q_h\right) = \left(\psi_h^{k+1} + p_h^{\star,k+1} - \nu \nabla \cdot \boldsymbol{u}_h^{k+1}, q_h\right), \quad \forall q_h \in M_h. \tag{4.7}$$

To investigate the compatibility between X_h and M_h, one only has to look at steady state solutions of the above algorithm. It is clear that any steady-state solution is such that $D\boldsymbol{u}_h^{k+1} = 0$, $\psi^{k+1} = 0$ and $p_h^{\star,k+1} = p_h^{k+1}$; as a result, the quantity $(\nabla \cdot \boldsymbol{u}_h^{k+1}, q_h)$ is zero for all q_h in M_h. In other words, the couple (u_h^{k+1}, p_h^{k+1}) is solution to the steady-state Stokes problem (4.2). Thus, although one can always determine a *unique* approximate solution $(\boldsymbol{u}_h^{k+1}, \psi_h^{k+1}, p_h^{k+1})$ from (4.5)–(4.7) with any triplet (X_h, W_h, M_h), there is no guaranty that the pressure approximation p_h^{k+1} does not contain any spurious mode in Q_h. In conclusion, for the schemes (2.10)–(2.12), the pair of spaces (X_h, M_h) has to satisfy the inf-sup condition for the pressure approximation to be free of spurious modes, and (except for spectral approximations, [1]) the inf-sup constant c_h should preferably be uniformly bounded from below for the pressure approximation to have optimal accuracy in space.

4.2. Full discretization of (2.8) and (2.9)

We now consider the schemes (2.8) and (2.9). Let $X_h \subset H^2(\Omega) \cap H_0^1(\Omega)^d$ and $M_h \subset H^1(\Omega)$ be respectively the approximation spaces for $\boldsymbol{u}_h^{k+1}$ and p_h^{k+1}. Then, a fully discretized version of (2.8) and (2.9) is: Find $(\boldsymbol{u}_h^{k+1}, p_h^{k+1}) \in X_h \times M_h$ such that

$$\left(\frac{D\boldsymbol{u}_h^{k+1}}{\Delta t}, \boldsymbol{v}_h\right) + \nu\left(\nabla \boldsymbol{u}_h^{k+1}, \nabla \boldsymbol{v}_h\right) - \left(p_h^{\star,k+1}, B_h \boldsymbol{v}_h\right) = \left(\boldsymbol{g}^{k+1}, \boldsymbol{v}_h\right), \quad \forall \boldsymbol{v}_h \in X_h, \tag{4.8}$$

$$\left(\nabla p_h^{k+1}, \nabla q_h\right) = \left(\boldsymbol{g} - \nu \nabla \times \nabla \times \boldsymbol{u}_h^{k+1}, \nabla q_h\right), \quad \forall q_h \in W_h. \tag{4.9}$$

Thus, the steady-state solution $(\boldsymbol{u}_h^{k+1}, p_h^{k+1}) \to (\boldsymbol{u}_h, p_h)$ satisfies the following *coupled* system:

$$\begin{aligned} &\nu(\nabla \boldsymbol{u}_h, \nabla \boldsymbol{v}) - (p_h, \nabla \cdot \boldsymbol{v}) = (\boldsymbol{g}, \boldsymbol{v}), \ \forall \boldsymbol{v} \in X_h, \\ &(\nabla p_h, \nabla q_h) = (\boldsymbol{g} - \nu \nabla \times \nabla \times \boldsymbol{u}_h, \nabla q_h), \ \forall q_h \in M_h. \end{aligned} \tag{4.10}$$

Numerical experiments with Legendre–Galerkin approximations [21] suggest that this system is well-posed for two set of spaces $X_h \times M_h$ such that one satisfies the inf-sup condition while the other does not (see Section 5). In other words, (4.10) does not seem to require a non trivial inf-sup condition to be satisfied for a unique solution to exist. In conclusion, we conjecture that the scheme (2.8) and (2.9) does not require the inf-sup condition to be satisfied.

5. Numerical experiments

To demonstrate the accuracy of the new splitting schemes, we perform convergence tests with respect to Δt with finite elements [10] and Legendre–Galerkin approximations [21].

5.1. Convergence tests with finite elements

We first test the finite element approximation on the time-dependent problem 1.1 in $\Omega =]0, 1[^2$. We set the source term so that the exact solution is

$$\begin{aligned} p(x,y,t) &= \cos(\pi x)\sin(\pi y)\sin t, \\ \boldsymbol{u}(x,y,t) &= (\pi\sin(2\pi y)\sin^2(\pi x)\sin t, -\pi\sin(2\pi x)\sin^2(\pi y)\sin t). \end{aligned} \tag{5.1}$$

We use mixed $\mathbb{P}_2/\mathbb{P}_1$ finite elements. The mesh used in the tests is composed of 14774 triangles so that the mesh size is $h \approx 1/80$. There are 7548 $\mathbb{P}_1$-nodes and 29869 $\mathbb{P}_2$-nodes. We make the tests on the range $5.10^{-4} \leqslant \Delta t \leqslant 10^{-1}$ so that the approximation error in space is far smaller than the time splitting error.

We have tested the algorithms (2.4)–(2.7) and (2.10)–(2.12) with $q = 2$.

The error on the velocity in the L^2-norm and in the H^1-norm at the final time, $T = 1$, is reported in Fig. 1 as a function of Δt. The results corresponding to the standard form of the algorithm are reported in the left panel of the figure, and those corresponding to the rotational form are in the right panel. The standard form of the algorithm is second-order accurate in the L^2-norm, but the convergence rate in the H^1-norm is roughly $3/2$. One clearly observes in the right panel of the figure that the rotational form of the algorithm is second-order accurate both in the L^2-norm and the H^1-norm. Note that the saturations observed for very small time steps is due to the approximation error in space which becomes dominant for very small time steps.

We show in Fig. 2 the error on the pressure measured in the L^∞-norm for both versions of the algorithm. The results clearly show that the pressure approximation in standard form is only first-order, whereas in the rotational formulation it is truly second-order. The poor convergence rate in the standard form can be attributed to the presence of numerical boundary layers which are induced by the fact that the boundary condition enforced by the approximate pressure, namely $\partial_n(p^{k+1} - 2p^k + p^{k-1})|_\Gamma = 0$, is not consistent.

This convergence test is a compelling evidence that the rotational form of the new scheme is truly second-order is time, although the proof of this result is still out of reach.

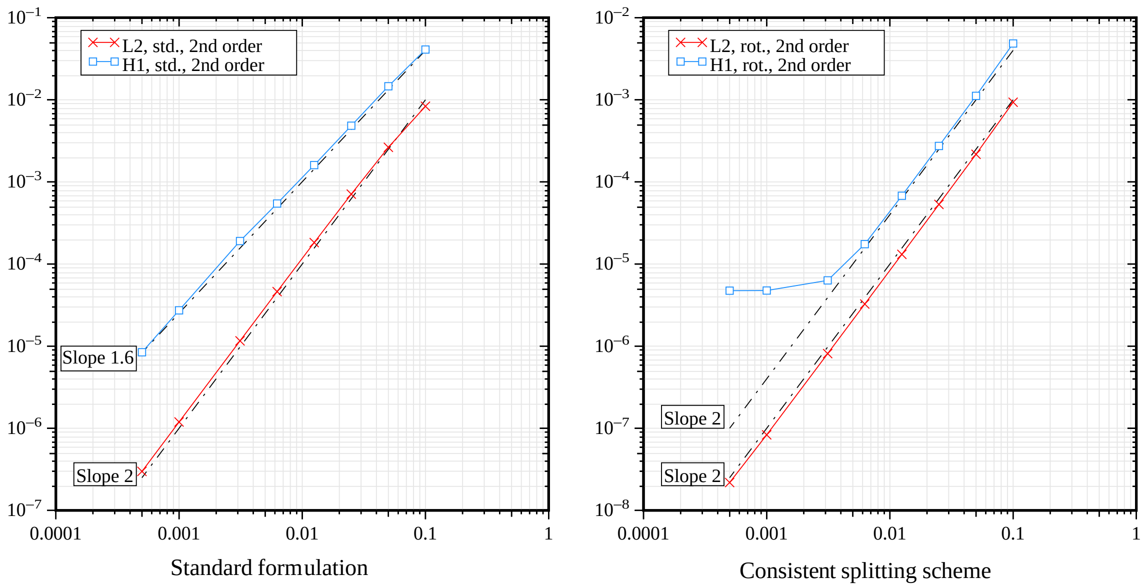

Fig. 1. Convergence tests with BDF2 and Finite elements. Error on the velocity in the L^2-norm and in the H^1-norm at $T = 1$. Standard formulation vs. consistent splitting scheme.

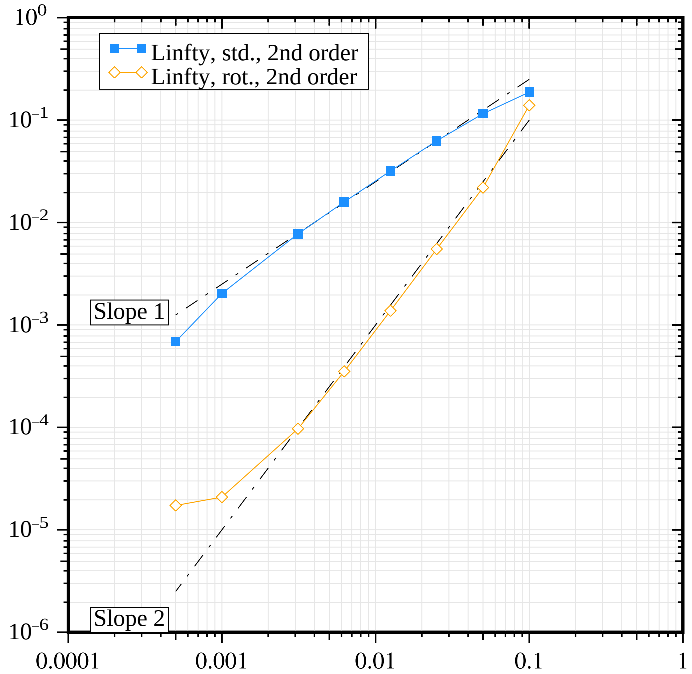

Fig. 2. Convergence tests with BDF2 and Finite elements. Error on the pressure in the L^∞-norm at $T = 1$. Standard formulation vs. rotational formulation.

5.2. Convergence tests with a Legendre–Galerkin approximation

We now present some tests using the Legendre–Galerkin method introduced in [21]. Let us denote by $\mathbb{P}_N$ the space of polynomials of degree less than or equal to N and $X_N = \{\boldsymbol{v} \in \mathbb{P}_N \times \mathbb{P}_N : \boldsymbol{v}|_\Gamma = 0\}$.

We have implemented both schemes (2.8) and (2.9) and (2.10)–(2.12) in $X_N \times \mathbb{P}_{N-2}$ and in $X_N \times \mathbb{P}_N$. Note that the set $X_N \times \mathbb{P}_N$ does not satisfy the inf-sup condition 4.3 of the Stokes problem while $X_N \times \mathbb{P}_{N-2}$ does. We have observed that the scheme (2.8) and (2.9) yields almost identical results with these two sets of spaces, whereas the scheme (2.10)–(2.12) yields spurious modes with $X_N \times \mathbb{P}_N$ but gives the same results as the other scheme with $X_N \times \mathbb{P}_{N-2}$. This set of tests confirms the observation made in Section 4, that is, the inf-sup condition (4.3) is needed for the scheme (2.10)–(2.12) to work properly, whilst it is not necessary for the scheme (2.8) and (2.9).

We now report convergence tests made with (2.10)–(2.12) in the polynomial setting $X_N \times \mathbb{P}_{N-2}$. We take the reference solution (5.1) in $\Omega = (-1, 1)^2$. We fix $N = 40$ so that the spatial discretization error is negligible when compared with the time discretization error.

In Fig. 3, we plot the errors on the pressure and the velocity measured in various norms as functions of the time step Δt. In the left panel we show the results form the splitting scheme in standard from, and in the right panel we show those from the consistent splitting scheme. These tests leave no doubts that the consistent splitting scheme provides full second-order accuracy for the velocity and the pressure in both the L^2- and H^1-norms. The results from the standard form of the splitting scheme are in full agreement with Theorem 3.1.

In Fig. 4, we plot the error field on the pressure at $t = 1$ using $\Delta t = 0.01$. On the left panel we show the error produced by the standard form of our splitting scheme, and in the right panel we show the field produced by the consistent splitting scheme. We observe that the error field produced by the standard form

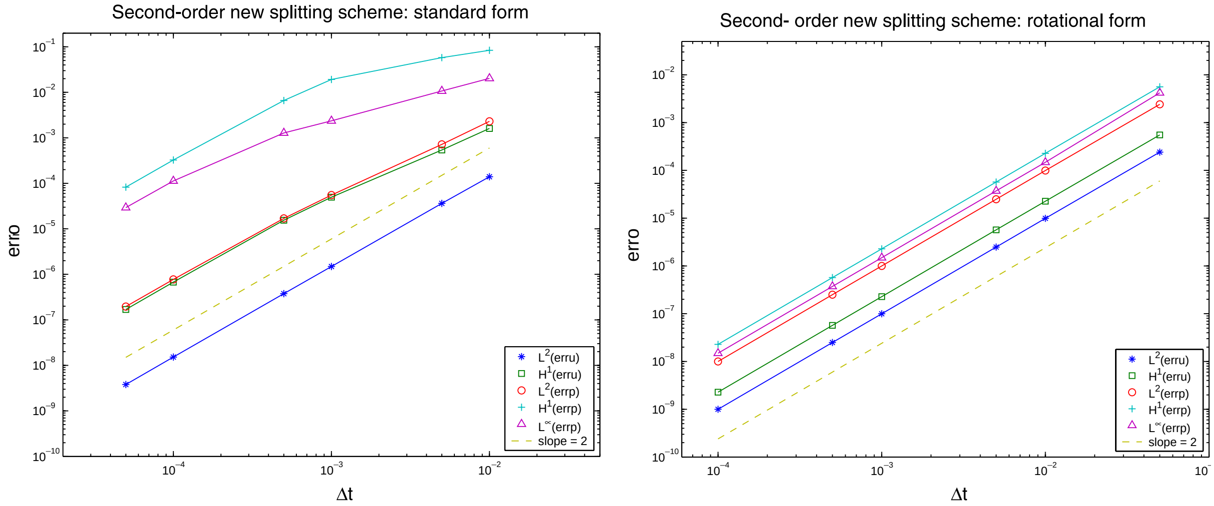

Fig. 3. Convergence rates with spectral approximation. $*$: velocity, L^2-norm; $\square$: velocity, H^1-norm; $\bigcirc$: pressure, L^2-norm; +: pressure, H^1-norm; $\triangle$: pressure, L^∞-norm. Standard formulation vs. consistent splitting scheme.

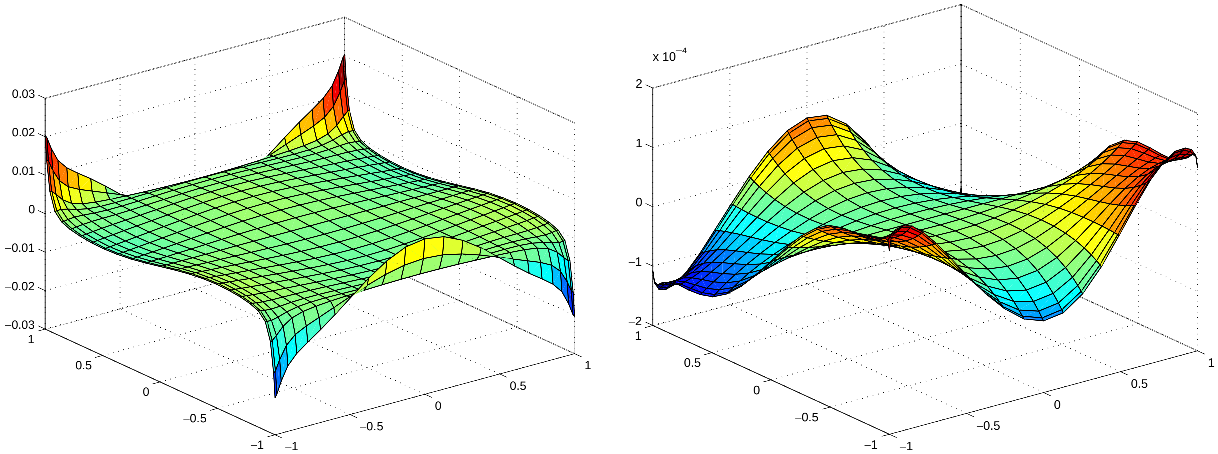

Fig. 4. Pressure error field at time $t = 1$ in a square. Standard formulation vs. consistent splitting scheme.

of the algorithm exhibits a numerical boundary layer. The presence of this numerical boundary layer is responsible for the loss of accuracy on the pressure and the vorticity. This phenomenon is comparable with what is observed for the standard form of pressure-correction schemes. Note that the error on the pressure produced by the consistent splitting scheme is smooth.

To complete this set of comparisons, we show in Fig. 5 the convergence rates and the error field on the pressure obtained by using the pressure-correction scheme in rotational form [13]. A comparison of these convergence rates illustrates clearly the significant improvement provided by the consistent splitting scheme over the rotational pressure-correction scheme. The lack of optimality of the rotational pressure-correction scheme is illustrated on the pressure error field by large spikes at the four corners of the domain.

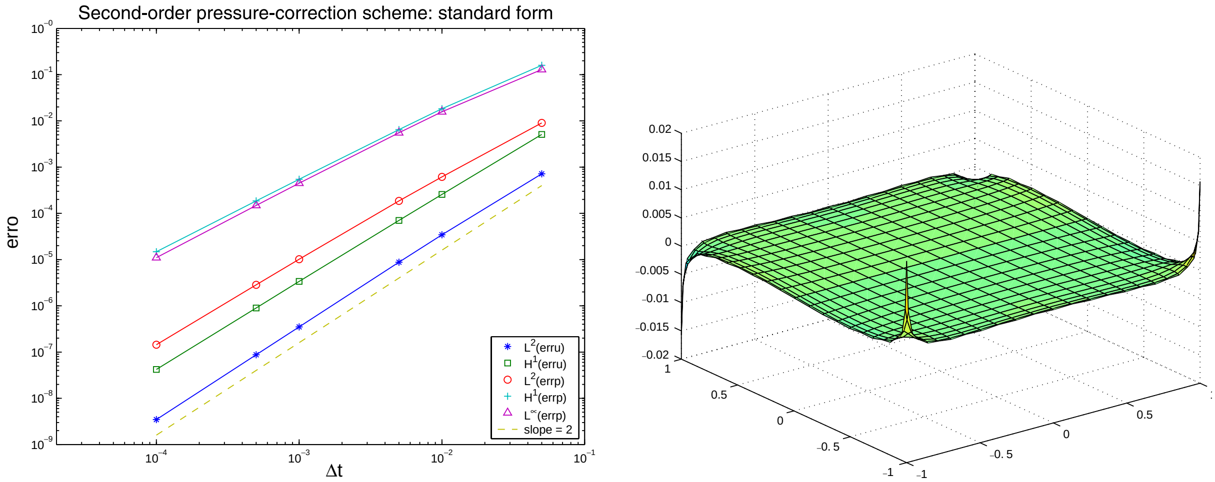

convergence rate pressure erroreld.

Fig. 5. Second-order rotational pressure-correction. ∗: velocity, L^2-norm; □: velocity, H^1-norm; ○: pressure, L^2-norm; +: pressure, H^1-norm; △: pressure, L^∞-norm. Convergence rate vs. pressure error field.

6. Concluding remarks

We have presented in this paper a new class of splitting schemes for incompressible flows. The new schemes are based on a weak form of the pressure Poisson equation, and at each time step, only require to solve a set of Helmholtz-type equations for the velocity and a Poisson equation (in the weak form) for the pressure.

Preliminary analysis and extensive numerical experiments have shown that the first-order (resp. second-order) consistent splitting schemes are unconditionally stable and yield full first-order (resp. second-order) accuracy for the velocity and the pressure in both L^2- and H^1-norms. Furthermore, if a discretization pair (X_h, M_h), e.g. a spectral or spectral-element discretization, allows for the implementation of the scheme (2.8) and (2.9), then optimal accuracy in space can be achieved even if (X_h, M_h) does not satisfy the inf-sup condition of the Stokes problem.

Thus, the second-order consistent splitting scheme enjoys many desirable properties such as decoupling, unconditionally stability, truly second-order accuracy (for the velocity and the pressure in both L^2 and H^1 norms), and when it is possible to implement the scheme in the form of (2.8) and (2.9), the inf-sup condition is not required.

To conclude, the second-order consistent splitting scheme appears to be a promising tool for numerical simulations of incompressible flows.

References

[1] F. Auteri, J.-L. Guermond, N. Parolini, Role of the LBB condition in weak spectral projection methods, J. Comput. Phys. 174 (2001) 405–420.
[2] I. Babuška, The finite element method with Lagrangian multipliers, Numer. Math. 20 (1972/73) 179–192.
[3] F. Brezzi, On the existence, uniqueness and approximation of saddle-point problems arising from Lagrangian multipliers, Rev. Française Automat. Informat. Recherche Opérationnelle Sér. Rouge 8 (R-2) (1974) 129–151.
[4] D.L. Brown, R. Cortez, M.L. Minion, Accurate projection methods for the incompressible Navier–Stokes equations, J. Comput. Phys. 168 (2) (2001) 464–499.

[5] A.J. Chorin, Numerical solution of the Navier–Stokes equations, Math. Comp. 22 (1968) 745–762.
[6] W. E, J.G. Liu, Projection method I: Convergence and numerical boundary layers, SIAM J. Numer, Anal. 32 (1995) 1017–1057.
[7] W. E, J.G. Liu, Gauge method for viscous incompressible flows, Comm. Math. Sci., 1, 2003.
[8] K. Goda, A multistep technique with implicit difference schemes for calculating two- or three-dimensional cavity flows, J. Comput. Phys. 30 (1979) 76–95.
[9] J.-L. Guermond, L. Quartapelle, On stability and convergence of projection methods based on pressure Poisson equation, Int. J. Numer. Methods Fluids 26 (9) (1998) 1039–1053.
[10] J.-L. Guermond, L. Quartapelle, On the approximation of the unsteady Navier–Stokes equations by finite element projection methods, Numer. Math. 80 (5) (1998) 207–238.
[11] J.-L. Guermond, Un résultat de convergence d'ordre deux en temps pour l'approximation des équations de Navier–Stokes par une technique de projection incrémentale, M2AN Math. Model. Numer. Anal. 33 (1) (1999) 169–189;
Also in J.-L. Guermond, C.R. Acad. Sci. Paris Série I 325 (1997) 1329–1332.
[12] J.L. Guermond, J. Shen, Error estimates for a new class of splitting schemes for incompressible flows, in preparation.
[13] J.L. Guermond, J. Shen, On the error estimates of rotational pressure-correction projection methods. Math. Comp. (2003), accepted.
[14] J.L. Guermond, J. Shen, Quelques résultats nouveaux sur les méthodes de projection, C.R. Acad. Sci. Paris, Série I 333 (2001) 1111–1116.
[15] J.L. Guermond, J. Shen, Velocity-correction projection methods for incompressible flows, SIAM J. Numer. Anal. 41 (1) (2003) 112–134.
[16] G.E. Karniadakis, M. Israeli, S.A. Orszag, High-order splitting methods for the incompressible Navier–Stokes equations, J. Comput. Phys. 97 (1991) 414–443.
[17] G.E. Karniadakis, S.J. Sherwin, Spectral/hp Element Methods for CFD, Oxford University Press, Oxford, 1999.
[18] J. Kim, P. Moin, Application of a fractional-step method to incompressible Navier-Stokes equations, J. Comput. Phys. 59 (1985) 308–323.
[19] S.A. Orszag, M. Israeli, M. Deville, Boundary conditions for incompressible flows, J. Sci. Comput. 1 (1986) 75–111.
[20] J. Shen, A remark on the projection-3 method, Int. J. Numer. Methods Fluids 16 (1993) 249–253.
[21] J. Shen, Efficient spectral-Galerkin method. i. Direct solvers of second- and fourth-order equations using Legendre polynomials, SIAM J. Sci. Comput. 15 (6) (1994) 1489–1505.
[22] J. Shen, On error estimates of projection methods for the Navier-Stokes equations: second-order schemes, Math. Comp. 65 (215) (1996) 1039–1065.
[23] J.C. Strikwerda, Y.S. Lee, The accuracy of the fractional step method, SIAM J. Numer. Anal. 37 (1) (1999) 37–47.
[24] R. Temam, Sur l'approximation de la solution des équations de Navier–Stokes par la méthode des pas fractionnaires ii, Arch. Rat. Mech. Anal. 33 (1969) 377–385.
[25] R. Temam, Navier–Stokes Equations: Theory and Numerical Analysis, North-Holland, Amsterdam, 1984.
[26] L.J.P. Timmermans, P.D. Minev, F.N. Van De Vosse, An approximate projection scheme for incompressible flow using spectral elements, Int. J. Numer. Methods Fluids 22 (1996) 673–688.
[27] J. van Kan, A second-order accurate pressure-correction scheme for viscous incompressible flow, SIAM J. Sci. Stat. Comput. 7 (3) (1986) 870–891.